HHS Public Access

Author manuscript

Nucl Med Biol. Author manuscript; available in PMC 2019 July 01.

Published in final edited form as:

Nucl Med Biol. 2018 ; 62-63: 71–77. doi:10.1016/j.nucmedbio.2018.06.001.

Matched-pair, ^{86}Y/^{90}Y-labeled, Bivalent RGD/Bombesin Antagonist, [RGD-Glu-[DO3A]-6-Ahx-RM2], as a Potential Theranostic Agent for Prostate Cancer

Nilantha Bandara[1], **Tamila J. Stott Reynolds**[2,6], **Rebecca Schehr**[7], **Rajendra P. Bandari**[3], **Philipp J. Diebolder**[1], **Stephanie Krieger**[1], **Jingli Xu**[5], **Yubin Miao**[5], **Buck E. Rogers**[1,*], and **Charles J. Smith**[2,3,4,*]

[1]Department of Radiation Oncology, Washington University School of Medicine, St. Louis, MO United States, 63108

[2]Research Division, Harry S. Truman Memorial Veterans' Hospital, Columbia, Missouri, United States, 65201

[3]Department of Radiology, University of Missouri School of Medicine, Columbia, MO, United States, 65211

[4]University of Missouri Research Reactor Center, University of Missouri, Columbia, MO, United States, 65211

[5]Department of Radiology, School of Medicine, University of Colorado Denver Aurora, CO, United States, 80045

[6]Department of Veterinary Pathobiology, Comparative Medicine Program, University of Missouri College of Veterinary Medicine, Columbia, MO, United States, 65211

[7]Veterinary Research Scholars Program, University of Missouri College of Veterinary Medicine, Columbia, MO, United States, 65211

Abstract

Introduction—In this study, we describe development of a true matched-pair theranostic agent that is able to target the $\alpha_V\beta_3$ integrin and the gastrin releasing peptide receptor (GRPR). We herein describe methods to metallate and characterize the new conjugate and to validate its biological efficacy by *in vitro* and *in vivo* methods.

Methods—We have previously described the development of [RGD-Glu-6Ahx-RM2] (where RGD: Arg-Gly-Asp; Glu: glutamic acid; 6-Ahx: 6-amino hexanoic acid; RM2: (D-Phe-Gln-Trp-Ala-Val-Gly-His-Sta-Leu-NH2)) that has been conjugated to a DOTA (1,4,7,10-

*Authors to whom correspondence should be addressed: Dr. Charles J. Smith, Department of Radiology, University of Missouri School of Medicine, One Hospital Drive, Columbia, MO 65212, smithcj@health.missouri.edu, Phone: (573)814-6000 ext. 53683. Dr. Buck E. Rogers, Department of Radiation Oncology, Washington University School of Medicine, 660 S. Euclid Avenue, CB8224, St. Louis, MO 63110, b.rogers@wustl.edu Phone: (314)362-9787.

tetraazacyclododecane-1,4,7,10-tetraacetic acid) bifunctional chelating agent (BFCA) to afford [RGD-Glu-[DO3A]-6-Ahx-RM2] peptide. In this study, we have radiolabeled [RGD-Glu-[DO3A]-6-Ahx-RM2] peptide with ^{86}Y or ^{90}Y. Natural-metallated (^{nat}Y) conjugates were assessed for binding affinity for the $\alpha_V\beta_3$ integrin or GRPR in human glioblastoma U87-MG and prostate PC-3 cell lines, respectively. The effective stability of the new tracers was also evaluated prior to *in vivo* evaluation in normal CF-1 mice and SCID mice bearing xenografted tumors.

Results—Competitive displacement binding assays in PC-3 cells showed high binding affinity for the GRPR (IC_{50}, 5.65 ± 0.00 nM). On the other hand, competitive displacement binding assays in U87-MG cells revealed only moderate binding to the $\alpha_V\beta_3$ integrin (IC_{50}, 346 ± 5.30 nM). Biodistribution studies in PC-3 tumor-bearing mice [RGD-Glu-[[^{90}Y]Y-DO3A]-6-Ahx-RM2] showed high tumor uptake (8.70 ± 0.35%ID/g at 1h post-intravenous injection) and retention of tracer (5.28 ± 0.12%ID/g) at 24h post-intravenous injection. Micro-positron emission tomography (microPET) in PC-3 tumor-bearing mice using [RGD-Glu-[^{86}Y]Y-DO3A]-6-Ahx-RM2] correlated well with biodistribution investigations over the various time points that were studied.

Conclusions—The [RGD-Glu-[[^{86}Y]Y-DO3A]-6-Ahx-RM2] and [RGD-Glu-[[^{90}Y]Y-DO3A]-6-Ahx-RM2] matched-pair conjugates described herein exhibit favorable microPET and pharmacokinetic profiles and merit further investigations for molecular imaging and/or therapeutic evaluation in larger animal models and potentially humans.

Advances in Knowledge and Implications for Patient Care—The theranostic, heterobivalent, agents described herein perform comparably with other mono- and multivalent conjugates we have reported and offer the potential of improved sensitivity for detecting prostate cancer cells that might exhibit differing profiles of receptor expression on tumor cells in human patients.

Keywords

Yttrium; prostate cancer; bombesin; RM2; RGD

1. Introduction

High-affinity GRPRs have been identified in tissue biopsy samples and immortalized cell lines of human prostate cancer and is an ideal biomarker for targeting early-stage disease [1–3]. In addition, radiolabeled peptides containing the amino acid sequence [Arg-Gly-Asp] are non-regulatory peptides that have been used extensively to target $\alpha_v\beta_3$ receptors upregulated on tumor cells and neovasculature, therefore providing a molecular vehicle for early detection of rapidly growing tumors and metastatic disease [4]. Therefore, the high incidence of expression of GRPRs and $\alpha_v\beta_3$-integrin on either early- or late-stage/metastatic prostate cancer disease creates a propensity for development of new and innovative bivalent radioligands to tailor receptor-specific uptake, optimize localization in cancerous tissues, and minimize uptake in normal tissues to produce high-quality, high-contrast PET/SPECT images for early diagnosis and staging of human prostate cancer and for the development of novel strategies for treatment of disease [5, 6].

We have previously described the development of [RGD-Glu-6Ahx-RM2] (where RGD: Arg-Gly-Asp; Glu: glutamic acid; 6-Ahx: 6-amino hexanoic acid; RM2: (D-Phe-Gln-Trp-

Ala-Val-Gly-His-Sta-Leu-NH2)) that has been conjugated to a DOTA (1,4,7,10-tetraazacyclododecane-1,4,7,10-tetraacetic acid) bifunctional chelating agent (BFCA) to produce [RGD-Glu-[DO3A]-6-Ahx-RM2] [6]. We have radiolabeled this novel agent with a variety of "theranostic" radionuclides that include ^{177}Lu, ^{111}In, and ^{67}Ga [6, 7]. In this study, we have radiolabeled [RGD-Glu-[DO3A]-6-Ahx-RM2] peptide with ^{86}Y and ^{90}Y to produce the new "matched-pair" tracer conjugate of the following general structure: [RGD-Glu-[[$^{90/86}$Y]Y-DO3A]-6-Ahx-RM2]. "Matched pairs" offer the unique opportunity to use information derived from routine patient diagnostic PET studies with ^{86}Y to determine the GRPR/$\alpha_v\beta_3$ availability on primary and metastatic tissues prior to administration of the corresponding therapeutic ^{90}Y analog. In this way, treatment would only be administered to patients previously demonstrating expression of the target receptor. Furthermore, the diagnostic radiopharmaceutical would be invaluable in pre-screening receptor-positive patients for therapy with respect to drug pharmacokinetics, receptor density, and patient dosimetry, potentially reducing or eliminating unsuccessful radiotherapeutic regimens. ^{86}Y and ^{90}Y are true "matched pairs" [8]. Their radiolabeling chemistries/dose preparations are identical. The pharmacokinetics and biodistribution of the ^{86}Y/^{90}Y-agents we are proposing should be altogether identical as well [9]. In addition, these new tracers offer the potential utility for monitoring patient dosimetry *via* a true "matched-pair" theranostic probe.

The rare-earth radionuclides decay by beta particle (β^-) emission and many are considered to be ideal in the context of targeted radiotherapy. The rare-earth isotopes exist primarily in the 3+ oxidation state and are considered to be hard metal centers, requiring multidentate, hard donor ligands for *in vivo* kinetic inertness [10]. ^{86}Y and ^{90}Y are considered to be rare-earth like elements in the context of radiolabeling and stability. For example, ^{86}Y and ^{90}Y require chelating, multidentate, poly(aminocarboxylates) such as DOTA to complex the metal center for *in vivo* kinetic inertness. ^{86}Y is a cyclotron-produced (Washington University, St. Louis, MO) [11], positron-emitting (β+, 32%) radionuclide that is prepared weekly. ^{86}Y has a sufficiently long-enough half-life (14.74 h) for shipping to be considered readily available for site-directed radiopharmaceutical preparation and PET molecular imaging. ^{86}Y is produced by irradiation of $^{86}SrCO_3$ or ^{86}SrO via the ^{86}Sr(p,n)^{86}Y nuclear reaction [12, 13]. ^{90}Y, on the other hand, is a pure β^--emitting (β_{max} = 2.381 MeV) radionuclide and is considered to be useful in the context of targeted radiotherapy. For example, the high energy β^- emitted by ^{90}Y could be ideal for deposition and irradiation of tumor tissue across many cellular cross sections. ^{90}Y has a physical half-life of 2.67 d and is commercially-available (Perkin Elmer) via the ^{90}Sr/^{90}Y generator system [14]. ^{90}Y has a penetrable range of ~5.7 mm in tissue, allowing for a cytotoxic delivery of radiation to both receptor-positive and potentially receptor-negative malignancies due to the crossfire effect [14].

2. Materials and Methods

2.1 General

The dimeric peptide conjugate, [Cyclo-(Arg-Gly-Asp-DTyr-Lys)-(DO3A)-Glu-(6-Ahx-D-Phe-Gln-Trp-Ala-Val-Gly-His-Sta-Leu-NH2)], [RGD-Glu-[DO3A]-6-Ahx-RM2], was a custom synthesis and was purchased from CPC Scientific (Sunnyvale, CA, USA). All other

reagents and solvents were purchased from Fisher Scientific (Pittsburgh, PA, USA) or Sigma-Aldrich Chemical Company (St. Louis, MO, USA). ^{125}I-[Tyr^4]-BBN was purchased from Perkin-Elmer (Waltham, MA, USA), and ^{125}I-Echistatin was purchased from Perkin Elmer, Inc. (Shelton, CT, USA). The human prostate adenocarcinoma (PC-3) and the human glioblastoma (U87-MG) cell lines were purchased from American Type Tissue Culture Center (ATCC, Rockland, MD) and the cells were maintained in 45% RPMI 1640, 45% Ham's F-12, and 10% heat-inactivated Fetal Bovine Serum (FBS). [^{86}Y]$YCl_3.3H_2O$ was produced by a (p,n) reaction on an enriched ^{86}Sr target[15] on the CS-15 biomedical cyclotron (Cyclotron Corporation, Berkeley, CA) at the Mallinckrodt Institute of Radiology, Washington University School of Medicine, St. Louis, MO. [^{90}Y]$YCl_3.3H_2O$ in 0.1M HCl solution was purchased from Perkin-Elmer (Billerica, MA, USA). All metallated and unmetallated peptide conjugates were purified *via* RP-HPLC performed on an SCL-10A HPLC system (Shimadzu, Kyoto, Japan) employing a binary gradient system [Solvent A=99.9% DI water with 0.1% trifluoroacetic acid (TFA); Solvent B=99.9% acetonitrile containing 0.1% TFA], programmed with a linear gradient of 30:70A/B to 20:80 A/B gradient over 15 min (followed by an additional 10 min at 10:90 A/B). Sample elution from an analytical-type, Proteo C-18 reversed-phase column (Phenomenex, Torrance, CA, USA) maintained at 34°C was monitored with an in-line Shimadzu SPD-10A absorption detector (λ=280 nm) and an in-line, EG&G Ortec NaI solid crystal scintillation detector (EG&G, Salem, MA, USA). Data acquisition of both signals was accomplished using EZStart software (7.4.3; Shimadzu, Kyoto, Japan). Purified compounds were lyophilized in a CentriVap system (Labconco, Kansas City, MO, USA). ESI-MS analyses were performed in the laboratory of Dr. Fabio Gallazzi at the University of Missouri, Department of Chemistry, Columbia, MO, USA.

2.2 Preparation of [RGD-Glu-[[$^{nat/90/86}$Y]Y-DO3A]-6-Ahx-RM2] conjugates

Metallation of [RGD-Glu-[DO3A]-6-Ahx-RM2] conjugate was based upon a previously published procedure [16] with only minor modifications. Brie y, natural $YCl_3.3H_2O$ in 0.05 N HCl (90 nmol) was added to puri ed [RGD-Glu-[DO3A]-6-Ahx-RM2] peptide conjugate (89 nmol) dissolved in 250 μL 0.4M ammonium acetate (NH_4OAc) and incubated at 80°C for a period of 1 h. Immediately after the 1h incubation period, 50 μL of 10 mM diethylenetriaminepentaacetic acid (DTPA) was added to the mixture to scavenge unbound metal. The resulting, metallated compound was puri ed by RP-HPLC and submitted for ESI-MS characterization prior to *in vitro* competitive binding assays. Similarly, synthesis of the new ^{90}Y radiotracer was achieved by the reaction of 50 μg of puri ed [RGD-Glu-[DO3A]-6-Ahx-RM2] (in 200 μL of 0.4 M NH_4OAc) with [^{90}Y]$YCl_3.3H_2O$ (37 MBq, ~1.8 x 10^{18} Bq/mol, 1 mCi, in 0.05 N HCl), followed by the addition of 50 μL of 10 mM DTPA solution to scavenge the remaining, unbound metal. The resulting radiotracer was purified by RP-HPLC and collected into 10 mg of ascorbic acid dissolved in 100 μL of 1 mg/mL bovine serum albumin (BSA) prior to *in vitro* stability assays and *in vivo* biodistribution investigations. Acetonitrile was removed under a steady stream of nitrogen and the radiochemical purity was assessed by RP-HPLC. [^{86}Y]$YCl_3.3H_2O$ was prepared at the Washington University School of Medicine. A stock solution of [^{86}Y]$YCl_3.3H_2O$ was obtained and diluted with a 10-fold excess of 0.1 M NH_4OAc, pH 7 for radiolabeling procedures. Radiolabeling of [RGD-Glu-[DO3A]-6-Ahx-RM2] with [^{86}Y]$YCl_3.3H_2O$ was achieved by addition of

[^{86}Y]$YCl_3.3H_2O$ (37 MBq, ~7.8 x 10^{18} Bq/mol, 1 mCi in 0.05 N HCl) to 50 μg of [RGD-Glu-[DO3A]-6-Ahx-RM2] in 100 μL of 0.1 M NH_4OAc. The solution was incubated on a thermomixer with 800 rpm agitation at 80ºC for 1 h. The resulting radiotracer was evaluated by RP-HPLC and used without further purification.

2.3 In vitro RP-HPLC stability assays

Ten microliters (~100 μCi) of [RGD-Glu-[[^{86}Y]Y-DO3A]-6-Ahx-RM2] was added to 90 μL of human serum (Sigma-Aldrich) and incubated at 37°C with agitation (300 rpm). Aliquots were removed at varying time points and analyzed by RP-HPLC. These studies were done in triplicate at 0.5, 1, 2, 4, 6, and 24 h time points. In addition, RP-HPLC-puri ed [RGD-Glu-[[^{90}Y]Y-DO3A]-6-Ahx-RM2] was collected into BSA and ascorbic acid and analyzed by RP-HPLC in order to assess the degree of product degradation due to radiolysis or radionuclide dissociation from the DO3A bifunctional chelating ligand. These investigations were performed at 0.5, 1, 2, 4, 6, and 24 h time points. All reactions were conducted in triplicate.

2.4 In vitro receptor binding assays for [RGD-Glu-[[^{nat}Y]Y-DO3A]-6-Ahx-RM2]

Half-maximum inhibitory concentration (IC_{50}) values for [RGD-Glu-[[^{nat}Y]Y-DO3A]-6-Ahx-RM2] were obtained in GRPR-expressing, human PC-3 prostate cancer cells (~ 1.5 x 10^6 cells/tube, suspended in DMEM/F-12K). Briefly, these studies were performed by incubation of ~20,000cpm of ^{125}I-[Tyr^4]-BBN (~3.18 x 10^{17} Bq/mol) and serial dilutions (10^{-5} M to 10^{-12} M) of [RGD-Glu-[[^{nat}Y]Y-DO3A]-6-Ahx-RM2] for 1 h at 37°C and 5% CO_2-enriched atmosphere. Following the incubation, media was aspirated and cells were washed three times in ice-cold buffer (pH 7, 0.2% BSA in DMEM+HEPES cell media). Cell-associated radioactivity was measured in a γ counter (Wallac Wizard 3” 1400, Perkin Elmer, Shelton, CT, USA) and generation of dissociation curves and calculation of IC_{50} values was done utilizing Prism 6 software. Assays were performed three times in triplicate. The binding affinity of [RGD-Glu-[[^{nat}Y]Y-DO3A]-6-Ahx-RM2] for the $\alpha_V\beta_3$ integrin was also determined *via* a competitive cell binding assay in $\alpha_V\beta_3$-expressing, human glioblastoma U87-MG cells using ^{125}I-Echistatin as the radioligand [16]. U87-MG cells (9 × 10^4 cells/well) were seeded in Millipore 96-well filter multiscreen DV plates (0.65μm pore size) and incubated at 25°C for 2 h with ~ 30,000 cpm of ^{125}I-Echistatin (~3.18 x 10^{17} Bq/mol) in the presence of increasing concentrations (10^{-12} M to 10^{-5} M) of [RGD-Glu-[[^{nat}Y]Y-DO3A]-6-Ahx-RM2] in 0.2 mL of binding medium. Plates were then filtered through a multiscreen vacuum manifold and rinsed twice with 0.5mL of ice-cold pH 7.4, 0.2% BSA/0.01M PBS. The hydrophilic polyvinylidenedifluoride (PVDF) filters were collected and the radioactivity was measured in a Wallac 2480 automated gamma counter (Perkin-Elmer, NJ). The IC_{50} values were calculated as previously described with assays being performed twice in triplicate.

2.5 In vivo biodistribution studies for [RGD-Glu-[[^{90}Y]Y-DO3A]-6-Ahx-RM2]

All animal studies were conducted in compliance with the highest standards of care as outlined in the NIH *Guide for the Care and Use of Laboratory Animals* (8th ed.) and the Policy and Procedures for Animal Research at the Truman VA Hospital, Columbia, Missouri, USA. Male, 4–5 week-old Institute of Cancer Research severe combined

immunodeficient (ICR-SCID) mice (Taconic Farms, Germantown, NY, USA) were utilized for these studies. Mice were housed four per cage in sterile, microisolator cages under temperature- and humidity-controlled conditions with a 12 h light/12 h dark schedule and fed autoclaved rodent chow (Ralston Purina 300 Company, St. Louis, MO, USA) and acidified water *ad libitum*. In preparation for tumor cell inoculations, SCID mice were anesthetized with isoflurane (Baxter Healthcare Corp., Deerfield, IL, USA) at an induction rate of 4% and maintained at a rate of 2.5% with 0.4 L oxygen delivered *via* precision vaporizer and a non-rebreathing apparatus. These mice received bilateral, subcutaneous rear flank injections of approximately 5 x 10^6 PC-3 cells suspended in 100 μL of 0.9% NaCl. Xenografted tumors were allowed to grow for ~5 weeks post-inoculation and ranged in mass from 0.03 g to 0.80 g. Biodistribution studies in male SCID mice were performed by tail vein injection of RP-HPLC-puri ed [RGD-Glu-[[^{90}Y]Y-DO3A]-6-Ahx-RM2] (20μCi, 1.8 x 10^{18} Bq/mol, 100 μL of 0.9% NaCl). Mice were sacrificed at 1, 4, or 24 h post-injection for harvest of tissues/organs (to include heart, lung, liver, kidneys, spleen, stomach, small intestine, large intestine, muscle, bone, brain, pancreas, blood, and tumor) and urine. At these specific time points, the urinary bladder was excised and counted along with cage paper in order to obtain an accurate assessment of urinary bladder radioactivity. Samples were subsequently weighed and counted without further processing in a NaI well counter (ORTEC EG&G, Oak Ridge, TN, USA). The percent injected dose (%ID) and the percent injected dose per gram (%ID/g) were calculated for all samples, with whole blood volume assumed to be 6.5% of the total body weight to allow for the %ID calculation in whole blood.

2.6 Autoradiography investigations using [RGD-Glu-[[^{86}Y]Y-DO3A]-6-Ahx-RM2]

All animal experiments were performed in compliance with the Guidelines for Care and Use of Research Animals established by the Division of Comparative Medicine and the Animal Sciences Committee of Washington University School of Medicine. In these invesitigations, harvested fresh tumors and muscle sections from male SCID mice were immediately frozen by immersing in liquid nitrogen. Tissue sectioning was carried out using a whole-body cryomicrotome (Vibratome 8850). Briefly, the tissues were adhered to the metal block holder using Cryo-M-Bed embedding compound (A-M systems) and frozen at −30°C on a Vibratome Cold Snap. Tissues were cut into 20–40 μm sections and attached to adhesive glass slides (CFSA 1X, Leica Bio Systems). Tumor and muscle sections were then exposed to a phosphor imaging plate (GE Healthcare Life Sciences) for 12 –16 h and the plates were scanned using a phosphor imager plate scanner (Storm 840). The resulting images were processed using ImageQuant 5.2 (Molecular Dynamics) and ImageJ (v1.48, public domain) software.

2.7 microPET molecular imaging investigations using [RGD-Glu-[[^{86}Y]Y-DO3A]-6-Ahx-RM2]

Small animal PET/CT imaging studies were conducted at the Washington University School of Medicine in male SCID mice (n=5 per group) bearing subcutaneous PC-3 xenografted tumors on the axillary thorax. Approximately 3.70-4.05 MBq (100–150 μCi) of [RGD-Glu-[[^{86}Y]Y-DO3A]-6-Ahx-RM2] tracer was administrated to mice *via* tail vein injection. Blocking studies were conducted using intravenous injections of either 10 μg of Tyr^4-Bombesin (B1), a 1:1 mixture of Tyr^4-Bombesin and RGD (B2), or 10 μg of RGD (B3)

diluted in saline. Mice were anesthetized using 1–2% isofluorane/oxygen and imaged on an Inveon small animal PET/CT imaging system (Siemens Medical Solutions) at 1, 4 and 24 h post administration. Static images were collected for 10 min for the 1 h and 4 h images and for 20 min for the 24 h images. Images were reconstructed with the Maximum Aposteriory Probability (MAP) algorithm followed by CT co-registration using the Inveon Research Workstation image display software (Siemens Medical Solutions, Knoxville, TN).

3. Results and Discussion

[RGD-Glu-[DO3A]-6-Ahx-RM2] was prepared by custom synthesis and purchased from CPC Scientific as previously described [6] and used without further purification. [RGD-Glu-[[*Y]Y-DO3A]-6-Ahx-RM2] conjugates that have been described in this study were puri ed by RP-HPLC and used as previously described [5–7]. Macroscopic [RGD-Glu-[[^{nat}Y]Y-DO3A]-6-Ahx-RM2] and tracer [RGD-Glu-[[$^{90/86}$Y]Y-DO3A]-6-Ahx-RM2] conjugates were produced in very high yield (≥95%) as veri ed by quality control RP-HPLC chromatographic profiles. With the equipment and parameters used at the University of Missouri, the unmetallated bivalent ligand eluted with a retention time of 10.8 min. The $^{nat/90}$Y-labeled conjugates exhibited a slightly longer retention time of 11.3 min (Table 1). Tracer-level investigations performed at the Washington University School of Medicine indicated a radiochemical purity of 98 ± 2.1% for the [RGD-Glu-[[^{86}Y]Y-DO3A)-6-Ahx-RM2] tracer as determined by RP-HPLC analysis. The new ^{86}Y-labeled conjugate eluted with a retention time of 8.1 min (Table 1). The retention time of macroscopic, [RGD-Glu-[[^{nat}Y]Y-DO3A)-6-Ahx-RM2], was 7.9 min (Table 1). These results are not unexpected considering only minor differences in polarizability, charge density, and atomic mass for the new conjugates. Furthermore, similar RP-HPLC elution profiles for the [RGD-Glu-[[$^{nat/90/86}$Y]Y-DO3A]-6-Ahx-RM2] conjugates clearly demonstrate the structural similarity between the macroscopic and tracer level conjugates. These results clearly mirror similar lanthanide or “lanthanide-like” conjugates we have described in previous publications [5–7]. Experimental results for ESI-MS identification of the new macroscopic, bivalent agent were consistent with the calculated molecular weight, further supporting the identi cation and characterization of the conjugates (Table 1, Fig. 1).

It is important to note that the biological half-life of a tracer need be very similar to the physical half-life of the radionuclide. More importantly, it is ideal for the biological half-life of the tracer to be greater than the physical half-life of the radioisotope (i.e., within a couple physical half-lives). The stability of [RGD-Glu-[[$^{86/90}$Y]Y-DO3A]-6-Ahx-RM2] was also determined by RP-HPLC. For each of the two tracers, RP-HPLC chromatographic profiles indicated very good stability, with very little change in the chromatographic profiles during the 0–6 h time point evaluation period. Very minor variation (noted by very subtle widening of the peak with accompanying decrease in amplitude) is seen at the 24 h time point for the ^{90}Y-conjugate, likely representing an effect from mild, radiolytic degradation of the otherwise pure, radiolabeled conjugate (Fig. 2). For the ^{86}Y-conjugate, essentially no unbound metal was observed over the evaluation time period indicating that the DO3A monoamide complex remained intact up to 24 h (Data not shown). Nonetheless, the results presented herein are clearly similar to other bivalent tracers we have evaluated in the past

and indicate sufficient stability for *in vivo* usage of these new theranostic probes in an animal model.

In vitro competitive binding studies for unmetallated [RGD-Glu-[DO3A]-6-Ahx-RM2] and metallated [RGD-Glu-[[^{nat}Y]Y-DO3A)-6-Ahx-RM2] conjugates were evaluated in PC-3 and U87-MG cells as previously described [5, 17]. The average IC_{50} was in the single-digit, nanomolar range for each [RGD-Glu-[DO3A]-6-Ahx-RM2] and [RGD-Glu-[[^{nat}Y]Y-DO3A)-6-Ahx-RM2] when evaluated in PC-3 cells (Table 1). On the other hand, [RGD-Glu-[DO3A]-6-Ahx-RM2] and [RGD-Glu-[[^{nat}Y]Y-DO3A]-6-Ahx-RM2] exhibited only moderate binding affinity and IC_{50} values of ~350nM when evaluated in $\alpha_v\beta_3$ integrin containing U87-MG glioblastoma cells (Table 1). [RGD-Glu-[^{nat}Y]Y-DO3A]-6-Ahx-RM2] exhibited a typical sigmoidal curve, depicting a dose-dependent response when performed in PC-3 and U87-MG cells (Fig. 3 and 4). The IC_{50} values re ect ef cient displacement of the competing radioligands (^{125}I-[Tyr4]-BBN or ^{125}I-Echistatin) with increasing concentrations of [RGD-Glu-(^{nat}Y-DO3A)-6-Ahx-RM2] conjugate. These results are altogether similar to those produced by our research group and others for similar, bivalent, GRPR/$\alpha_v\beta_3$-targeting agents [5, 6, 18–21].

In order to determine the relative uptake and retention of tracer in tumor tissue, biodistribution investigations were performed in male SCID mice bearing PC-3 xenografted tumors. Biodistribution data for [RGD-Glu-[[^{90}Y]Y-DO3A]-6-Ahx-RM2] are listed in Table 2. The primary mode of excretion for [RGD-Glu-[[^{90}Y]-DO3A]-6-Ahx-RM2] was the renal-urinary pathway. For example, average urine radioactivity excretion of 93.4% ± 1.26% ID was observed by 4 h post-injection. To evaluate the stability of the [RGD-Glu-[[^{90}Y]Y-DO3A]-6-Ahx-RM2] tracer *in vivo*, we were able to collect the urine and examine it by RP-HPLC. The urinary radioactivity eluted with a similar retention time (~11.2 min) as the original tracer, suggesting structural similarity between the two species. Effective clearance from renal tissue in the tumor-bearing mice (2.36±0.49% ID/g at 1h, 1.54±0.31% ID/g at 4h and 0.89±0.21% ID/g at 24h) were superior to those seen previously for [RGD-Glu-[[^{177}Lu]Lu-DO3A]-6-Ahx-RM2] in the same tumor model (4.32±2.17% ID/g at 1h, 2.37±0.77% ID/g at 4h, 1.57±0.44% ID/g at 24h). Similarly, high initial uptake and retention in kidney was also observed for [RGD-Glu-[[^{111}In]In-DO3A]-6-Ahx-RM2] (3.74±0.60% ID/g at 1h, 2.33±0.50% ID/g at 4h, 1.12±0.63% ID/g at 24h) tracer that was previously reported by our research group [6]. In contrast to the ^{177}Lu and ^{111}In agents we have described, hepatic accumulation was decreased for the [RGD-Glu-[[^{90}Y]Y-DO3A]-6-Ahx-RM2] in PC-3 tumor-bearing mice, with the ^{90}Y-conjugate showing only 0.39±0.08 % ID/g at 1 h, decreasing to 0.35±0.07% ID/g and 0.29±0.15% ID/g by 4 h and 24 h, respectively. Tracer retention in xenografted tumors was found to be higher at all time points for [RGD-Glu-[[^{90}Y]Y-DO3A]-6-Ahx-RM2] when compared to the [RGD-Glu-[[^{177}Lu}Lu-DO3A]-6-Ahx-RM2] and [RGD-Glu-[[^{111}In]In-DO3A]-6-Ahx-RM2]. For example, an average maximal concentration of 8.70±0.35% ID/g in tumor was observed at 1 h post-injection versus ~7% ID/g for the In and Lu tracers, respectively. In addition, the 1 h tumor uptake noted for [RGD-Glu-[[^{90}Y]Y-DO3A]-6-Ahx-RM2] exceeded that of all organs including the pancreas, which is known to express the GRPR in very high numbers [8, 22–24]. Overall, the [RGD-Glu-[[^{90}Y]Y-DO3A]-6-Ahx-RM2] antagonist reported herein exhibits higher tumor retention than both [RGD-Glu-[[^{177}Lu]Lu-DO3A]-6-Ahx-RM2] and [RGD-Glu-

[[^{111}In]In-DO3A]-6-Ahx-RM2] bivalent radioligands, demonstrating not only a higher initial accumulation of tracer in tumor tissue, but also a higher residual retention of radioactivity than either of the comparable ^{177}Lu or ^{111}In heterodimers at the 24 h time points. Results of ex vivo autoradiography (Figure 5) and also blocking investigations in tumor with Tyr^4-bombesin indicate that the predominant receptor-binding mechanism is by the RM2 motif on the GRPR, with little discernible contribution from the RGD-targeting portion of the ligand for $\alpha_v\beta_3$ integrin.

Evaluation of data in target (tumor) and non-target tissues are an important measure of a radiopharmaceutical's potential diagnostic and/or therapeutic utility. For example, an analysis of this data can be most useful as a point of comparison with other similar tracers targeting a particular cell line of interest. The tumor to non-target tissue ratio data for [RGD-Glu-[[^{90}Y]Y-DO3A]-6-Ahx-RM2] is also shown in Table 2. It is clearly evident that this new tracer exhibits tumor to non-target ratios conducive to high-quality, high-contrast molecular imaging (as exhibited in microPET imaging investigations) or possibly even radiotherapy. The kidneys, and in particular, the pancreas (which is expected to also express the GRPR), exhibit lower tumor-to-non-tumor uptake ratios than those of non-GRPR-expressing tissues such as muscle and bone. The liver showed very reasonable ratios at all time points post-injection, superior to either [RGD-Glu-[[^{177}Lu]Lu-DO3A]-6-Ahx-RM2] or [RGD-Glu-[[^{111}In]In-DO3A]-6-Ahx-RM2].

The results of microPET/microCT imaging studies in PC-3 tumor-bearing, SCID mice following injection with [RGD-Glu-[[^{86}Y]Y-DO3A]-6-Ahx-RM2] and blocking agents are presented in Figure 6. Xenografted tumors were clearly discernible from all other tissues at all time points, with very little background retention in non-tumor tissue other than kidneys and bladder, owing to the rapid urinary clearance that was also observed in the biodistribution investigations. In order to establish the *in vivo* specificity of [RGD-Glu-[[^{86}Y]Y-DO3A]-6-Ahx-RM2], blocking investigations were performed with three blocking strategies (B1, B2, and B3) as described Materials and Methods. In the presence of 100% Tyr^4-bombesin (B1), radiolabeled signal was suppressed in the tumor and in other tissues where GRPR presence is to be expected. A mixture of blocking agents (B2) resulted in nearly complete blocking of both the RM2 and RGD ligands at all time points. However, addition of 100% RGD (B3) as the blocking agent demonstrated some uptake/retention of tracer at all time points according to the microPET images. Results of these studies indicate that PC-3 tumor expression of the GRPR is much greater than expression of the $\alpha_v\beta_3$ integrin, as we and others have previously reported [5, 6, 25]. MicroPET images using [RGD-Glu-[[^{86}Y]Y-DO3A]-6-Ahx-RM2] tracer correlate well with biodistribution data (Table 2) for the corresponding ^{90}Y-conjugate. For example, tumor tissue exhibited the highest uptake in tissues with some accumulation in the kidneys at 1 h. However, renal clearance of tracer was evident at 4 h, and was nearly complete by the 24 h time point in the non-blocked image (Fig. 6).

4. Conclusion

Recent developments in bivalent, tracer-level technology include clinical investigations of ^{68}Ga-NOTA-BBN-RGD in a select group of prostate cancer patients. Those studies

represent the first “in-human” clinical investigations for novel agents of the type we have described [26]. Those authors have demonstrated the safety and efficiency of using a ^{68}Ga-radiolabeled dual $\alpha_v\beta_3$ integrin and GRPR targeting agent for PET molecular imaging of patients presenting with primary or metastatic disease. In fact, in 13 patients with prostate cancer determined by needle biopsy, ^{68}Ga-NOTA-BBN-RGD was able to detect 3 of 4 primary tumors, 14 metastatic lymph node lesions, and 20 bone metastases [26].

In the current study, we have evaluated the true “matched-pair” tracers [RGD-Glu-[[^{86}Y]Y-DO3A]-6-Ahx-RM2] and [RGD-Glu-[[^{90}Y]Y-DO3A]-6-Ahx-RM2]. These new tracers are akin to similar agents we have previously reported upon that include [RGD-Glu-[[^{111}In]In-DO3A]-6-Ahx-RM2] and [RGD-Glu-[[^{177}Lu]Lu-DO3A]-6-Ahx-RM2]. All of these new tracers were designed to target either the $\alpha_v\beta_3$ integrin or the GRPR, well-validated biomarkers found on most prostate cancer cells. MicroPET/CT images of mice injected with [RGD-Glu-[[^{86}Y]Y-DO3A]-6-Ahx-RM2] produced high-quality, high-contrast, whole-body images with minimal tracer present in non-tumor tissues at all validated time points described in this study. These imaging results, as well as those of the *in vivo* [RGD-Glu-[[^{90}Y]Y-DO3A]-6-Ahx-RM2] biodistribution investigations in tumor-bearing, SCID mice indicate that both of these new compounds exhibit high speci city and very good af nity for the GRPR in PC-3 tumors. Specific targeting of the integrin, appears to be to a lesser extent in this tumor model based clearly upon the relative expression of $\alpha_v\beta_3$ in the PC-3 cell line. Other tumors with alternate expression profiles for the targets GRPR and $\alpha_v\beta_3$ might allow for capture of a larger “audience” of biomarker-expressing tumors *in vivo*. None-the-less, albeit targeting of the $\alpha_v\beta_3$ integrin seems to be at a lesser extent than the GRPR, these data still suggest the new tracers to be potentially useful as a theranostic matched-pair for primary and metastatic prostate cancer. MicroPET imaging investigations showed some reduction in tracer retention for [RGD-Glu-[[^{90}Y]Y-DO3A]-6-Ahx-RM2] by the 24 h time point. However, tumor retention remained high at 24 h while retention in other non-target tissues was nearly nonexistent. An additional advantage of these new tracers is the potential utility for monitoring patient dosimetry *via* a true “matched-pair” theranostic probe. Biodistribution data for [RGD-Glu-[[^{86}Y]Y-DO3A]-6-Ahx-RM2] would be helpful for a more direct comparison to microPET molecular imaging data and to biodistribution data obtained for [RGD-Glu-[[^{90}Y]Y-DO3A]-6-Ahx-RM2] tracer. Furthermore, analysis of SUVs (standardized uptake values) and area-under-the-curve methods might also be useful for examining the therapeutic utility of these new tracers. However, overall, results from these studies support previous investigations from our labs and others suggesting the potential clinical utility of using radiolabeled heterodimeric ligands targeting more than one biomarker as agents for PET or SPECT molecular imaging and therapy.

Acknowledgments

This material was the result of work supported with resources and the use of facilities at the Harry S. Truman Memorial Veterans’ Hospital in Columbia (HSTMVH), MO, 65201 and the University of Missouri School of Medicine, Columbia, MO 65211, USA. Dr. Tamila Stott Reynolds acknowledges financial support from NIH T32 Grant #5T32OD011126-35. This work was also funded in part by The United States Department of Veterans’ Affairs, VA Merit Bridge Funding Award Mechanism and VA MERIT Application 1I01BX003392. The authors would also like to thank the Isotope Production Group at Washington University, St. Louis, MO, 63108, for production of $^{86}YCl_3.3H_2O$. We also acknowledge the Small Animal Imaging Facility at the Washington University School of Medicine, St. Louis, MO, 63108, for technical assistance during the microPET/CT molecular

imaging investigations. Nilantha Bandara would like to acknowledge financial support from the United States Department of Energy (DOE, BER, DE-SC0002032). Last of all, financial support from the Department of Radiation Oncology at Washington University is also gratefully acknowledged.

References

1. Markwalder R, Reubi JC. Gastrin-releasing peptide receptors in the human prostate: Relation to neoplastic transformation. Cancer Res. 1999; 59:1152–9. [PubMed: 10070977]
2. Pinski J, Halmos G, Yano T, Szepeshazi K, Qin Y, Ertl T, et al. Inhibition of growth of MKN45 human gastric-carcinoma xenografts in nude mice by treatment with bombesin/gastrin-releasing-peptide antagonist (RC-3095) and somatostatin analogue RC-160. Int J Cancer. 1994; 57:574–80. [PubMed: 7910153]
3. Sun B, Schally AV, Halmos G. The presence of receptors for bombesin/GRP and mRNA for three receptor subtypes in human ovarian epithelial cancers. Regulatory Peptides. 2000; 90:77–84. [PubMed: 10828496]
4. Liu S, Liu Z, Chen K, Yan Y, Watzlowik P, Wester HJ, et al. 18F-labeled galacto and PEGylated RGD dimers for PET imaging of αvβ3 integrin expression. Molecular Imaging and Biology. 2010; 12:530–8. [PubMed: 19949981]
5. Durkan K, Jiang Z, Rold TL, Sieckman GL, Hoffman TJ, Bandari RP, et al. A heterodimeric [RGD-Glu-[64Cu-NO2A]-6-Ahx-RM2] αvβ3/GRPr-targeting antagonist radiotracer for PET imaging of prostate tumors. Nuclear Medicine and Biology. 2014; 41:133–9. [PubMed: 24480266]
6. Stott Reynolds TJ, Schehr R, Liu D, Xu J, Miao Y, Hoffman TJ, et al. Characterization and evaluation of DOTA-conjugated Bombesin/RGD-antagonists for prostate cancer tumor imaging and therapy. Nuclear Medicine and Biology. 2015; 42:99–108. [PubMed: 25459113]
7. Jiang ZP, Bandari RJ, Stott Reynolds T, Xu J, Miao Y, Rold TL, et al. Molecular imaging investigations of a 67Ga/64Cu labeled bivalent ligand, [RGD-Glu-(DO3A)-6-Ahx-RM2], targeting GRPR/αvβ3 biomarkers: A comparative study. 2016
8. Biddlecombe GB, Rogers BE, De Visser M, Parry JJ, De Jong M, Erion JL, et al. Molecular imaging of gastrin-releasing peptide receptor-positive tumors in mice using 64Cu- and 86Y-DOTA-(Pro1,Tyr 4)-bombesin(1–14). Bioconjugate Chemistry. 2007; 18:724–30. [PubMed: 17378600]
9. Smith CJ, Gali H, Sieckman GL, Hayes DL, Owen NK, Mazuru DG, et al. Radiochemical investigations of 177Lu-DOTA-8-Aoc-BBN[7-14]NH2: An in vitro/in vivo assessment of the targeting ability of this new radiopharmaceutical for PC-3 human prostate cancer cells. Nuclear Medicine and Biology. 2003; 30:101–9. [PubMed: 12623108]
10. Cutler CS, Smith CJ, Ehrhardt GJ, Tyler TT, Jurisson SS, Deutsch E. Current and potential therapeutic uses of lanthanide radioisotopes. Cancer Biother Radio. 2000; 15:531–45.
11. Zovato S, Kumanova A, Dematte S, Sansovini M, Bodei L, Di Sarra D, et al. Peptide receptor radionuclide therapy (PRRT) with 177Lu-DOTATATE in individuals with neck or mediastinal paraganglioma (PGL). Horm Metab Res. 2012; 44:411–4. [PubMed: 22566197]
12. Bodei L, Cremonesi M, Grana CM, Chinol M, Baio SM, Severi S, et al. Yttrium-labelled peptides for therapy of NET. Eur J Nucl Med Mol Imaging. 2012; 39(Suppl 1):S93–102. [PubMed: 22388625]
13. Scalvini A, Ferrari V, Bodei S, Arcangeli G, Consoli F, Spano P, et al. Involvement of target gene polymorphisms in 5-Fluorouracil toxicity: a case report. Pharmacology. 2012; 89:99–102. [PubMed: 22343422]
14. Arrighi N, Bodei S, Zani D, Simeone C, Cunico SC, Spano PF, et al. Acetylcholine induces human detrusor muscle cell proliferation: molecular and pharmacological characterization. Urologia. 2012; 79:102–8. [PubMed: 22610841]
15. Yoo J, Tang L, Perkins TA, Rowland DJ, Laforest R, Lewis JS, et al. Preparation of high specific activity 86Y using a small biomedical cyclotron. Nuclear Medicine and Biology. 2005; 32:891–7. [PubMed: 16253815]
16. Durkan K, Jiang Z, Rold TL, Sieckman GL, Hoffman TJ, Bandari RP, et al. A heterodimeric [RGD-Glu-[(64)Cu-NO2A]-6-Ahx-RM2] alphavbeta3/GRPr-targeting antagonist radiotracer for PET imaging of prostate tumors. Nuclear medicine and biology. 2014; 41:133–9. [PubMed: 24480266]

17. Jiang L, Miao Z, Liu H, Ren G, Bao A, Cutler CS, et al. 177Lu-labeled RGD-BBN heterodimeric peptide for targeting prostate carcinoma. Nuclear Medicine Communications. 2013; 34:909–14. DOI: 10.1097/MNM.0b013e328362d2b6 [PubMed: 23708872]

18. Bhirde A, Xie J, Swierczewska M, Chen X. Nanoparticles for cell labeling. Nanoscale. 2011; 3:142–53. [PubMed: 20938522]

19. Liu Z, Li ZB, Cao Q, Liu S, Wang F, Chen X. Small-animal PET of tumors with ^{64}Cu-labeled RGD-bombesin heterodimer. J Nucl Med. 2009; 50:1168–77. [PubMed: 19525469]

20. Liu Z, Niu G, Wang F, Chen X. ^{68}Ga-labeled NOTA-RGD-BBN peptide for dual integrin and GRPR-targeted tumor imaging. E J Nucl Med and Mol Imag. 2009; 36:1483–94.

21. Liu Z, Yan Y, Chin FT, Wang F, Chen X. Dual integrin and gastrin-releasing peptide receptor targeted tumor imaging using18F-Labeled PEGylated RGD-bombesin heterodimer 18F-FB-PEG3-Glu-RGD-BBN. Journal of Medicinal Chemistry. 2009; 52:425–32. [PubMed: 19113865]

22. Nanda PK, Rold TL, Sieckman GL, Szczodroski AF, Hoffman TJ, Rogers BE, et al. Positron-emission Tomography (PET) Imaging Agents for Diagnosis of Human Prostate Cancer: Agonist Versus Antagonist Ligands. In Vivo. 2012; 26:583–92. [PubMed: 22773572]

23. Rogers BE, Bigott HM, McCarthy DW, Della Manna D, Kim J, Sharp TL, et al. MicroPET imaging of a gastrin-releasing peptide receptor-positive tumor in a mouse model of human prostate cancer using a 64Cu-labeled bombesin analogue. Bioconjugate Chem. 2003; 14:756–63.

24. Rogers BE, Manna DD, Safavy A. In Vitro and In Vivo Evaluation of a ^{64}Cu-Labeled Polyethylene Glycol-Bombesin Conjugate. Cancer Biother Radio. 2004; 19:25–34.

25. Liu S. Radiolabeled Cyclic RGD Peptides as Integrin αvβ3-Targeted Radiotracers: Maximizing Binding Affinity via Bivalency. Bioconjugate Chemistry. 2009; 20:2199–213. [PubMed: 19719118]

26. Zhang J, Niu G, Lang L, Li F, Fan X, Yan X, et al. Clinical translation of a dual integrin αvβ3 and GRPR targeting PET radiotracer 68Ga-NOTA-BBN-RGD. Journal of Nuclear Medicine. 2016

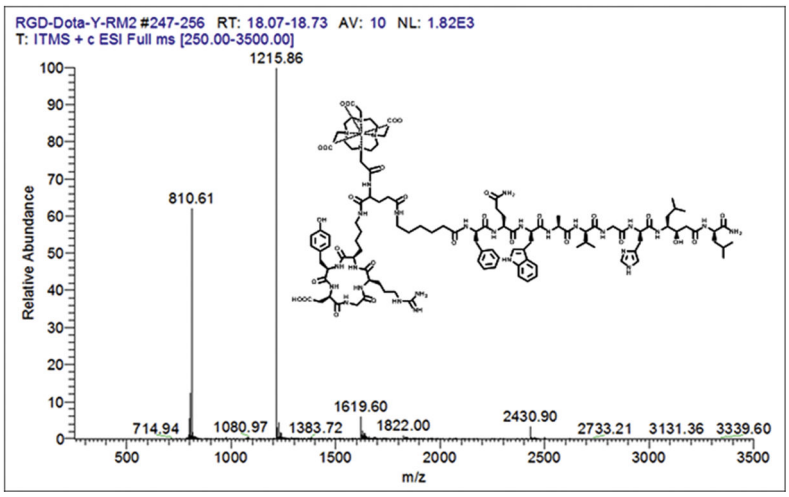

FIGURE 1.

Mass spectrum and chemical structure of [RGD-Glu-[[^{nat}Y]Y-DO3A]-6-Ahx-RM2].

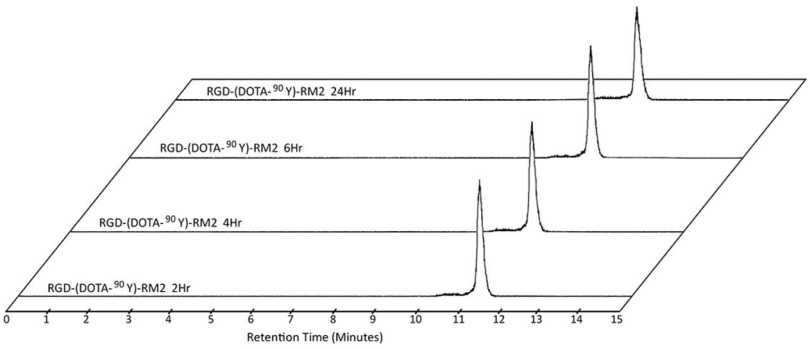

FIGURE 2.

HPLC chromatographic profiles in human serum for [RGD-Glu-[[^{90}Y]Y-DO3A]-6-Ahx-RM2].

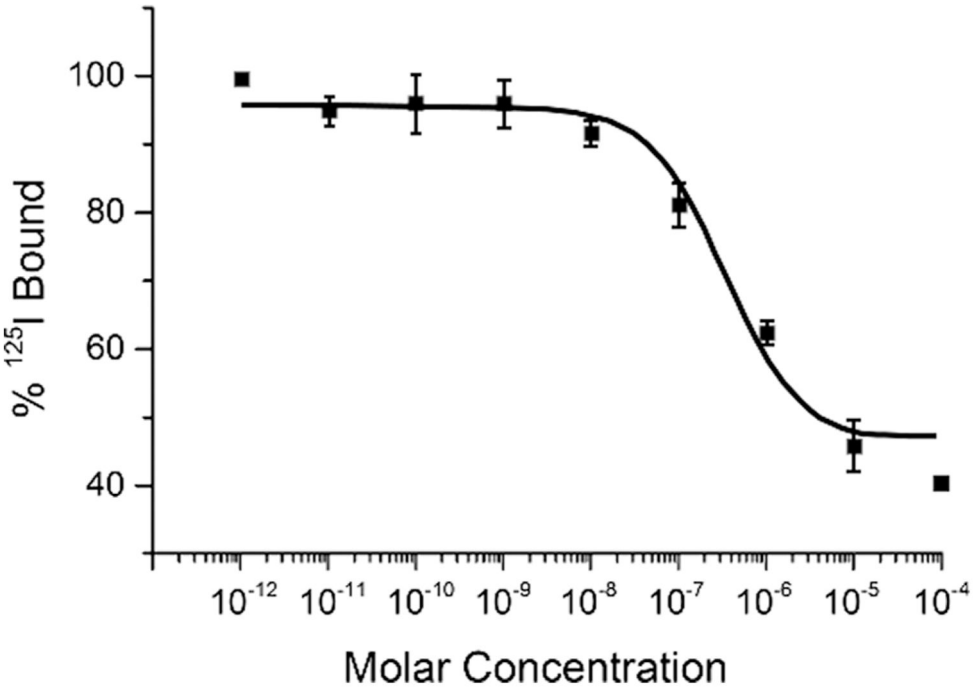

FIGURE 3.

Half-maximum inhibitory concentration (IC_{50}) for [RGD-Glu-[[^{nat}Y]Y-DO3A]-6-Ahx-RM2] (IC_{50} = 346±5.30 nM) in human, glioblastoma, U87-MG cells.

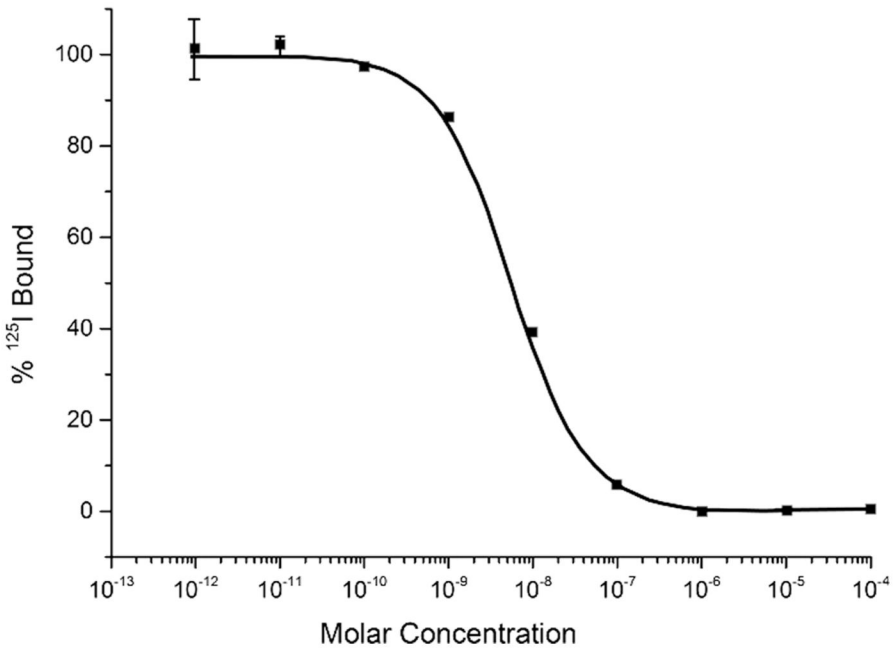

FIGURE 4.

Half-maximum inhibitory concentration (IC_{50}) for [RGD-Glu-[[^{nat}Y]Y-DO3A]-6-Ahx-RM2] (IC_{50} = 5.65±0.00 nM) in human, prostate, PC-3 cells.

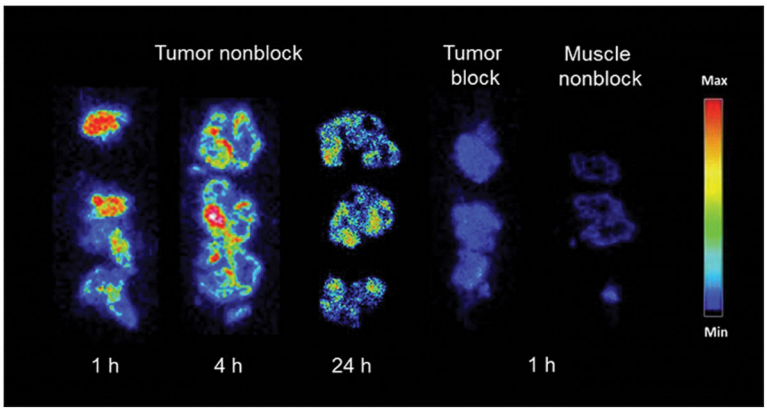

FIGURE 5.

Ex vivo autoradiography investigations in tumor, muscle, and blocked tumor using [RGD-Glu-[[^{86}Y]Y-DO3A]-6-Ahx-RM2].

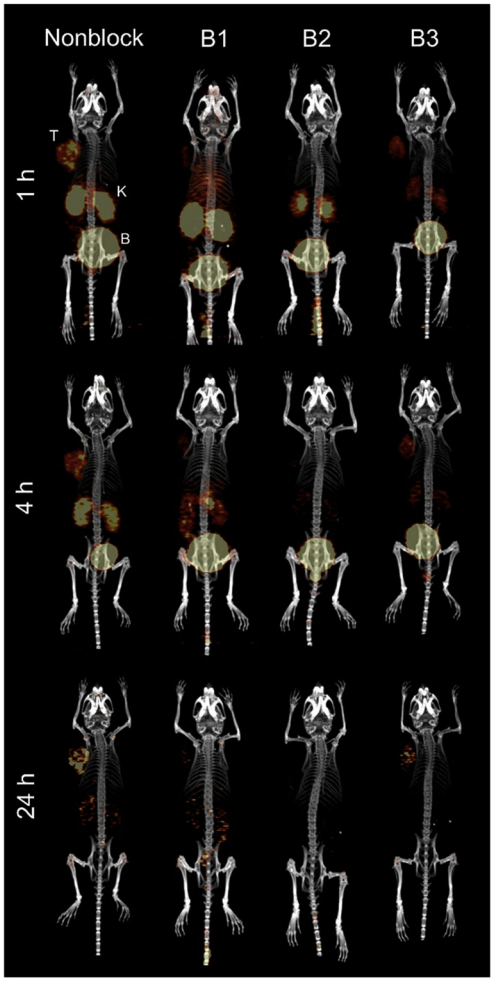

FIGURE 6.

Maximum intensity microPET tumor and microCT skeletal fusion coronal, whole-body images of PC-3 tumor-bearing SCID mice at 1 h, 4 h, and 24 h post-tail vein injection of [RGD-Glu-[[^{86}Y]Y-DO3A]-6-Ahx-RM2] and corresponding blocking agent (tumors (T), kidneys (K), and bladder (B)).

TABLE 1

Mass spectrometry, IC_{50}, and RP-HPLC data for [RGD-Glu-[DO3A]-6-Ahx-RM2] and [RGD-Glu-[[$^{nat/86/90}$Y]Y-DO3A]-6-Ahx-RM2].

Molecular Formula [RGD-Glu-[DO3A]-6-Ahx-RM2]	$C_{109}H_{163}N_{29}O_{29}$
Molecular Formula [RGD-Glu-[Y-DO3A]-6-Ahx-RM2]	$C_{109}H_{160}N_{29}O_{29}Y$
Calculated molecular mass, [RGD-Glu-[DO3A]-6-Ahx-RM2]	2343.64 Da
Calculated molecular mass, [RGD-Glu-[[^{nat}Y]Y-DO3A]-6-Ahx-RM2]	2429.56 Da
ESI-MS molecular mass, [RGD-Glu-[DO3A]-6-Ahx-RM2]	2344.86 Da
ESI-MS molecular mass, [RGD-Glu-[[^{nat}Y]Y-DO3A]-6-Ahx-RM2]	2430.90 Da
[RGD-Glu-[DO3A]-6-Ahx-RM2], RP-HPLC t_R	10.8 min
[RGD-Glu-[[^{nat}Y]Y-DO3A]-6-Ahx-RM2], RP-HPLC t_R	11.3 min
[RGD-Glu-[[^{86}Y]Y-DO3A]-6-Ahx-RM2], RP-HPLC t_R	11.2 min
[RGD-Glu-[[^{90}Y]Y-DO3A]-6-Ahx-RM2], RP-HPLC t_R	11.3 min
IC_{50}, [RGD-Glu-[DO3A]-6-Ahx-RM2], PC-3	9.26±0.01 nM
IC_{50}, [RGD-Glu-[[^{nat}Y]Y-DO3A]-6-Ahx-RM2], PC-3	5.65±0.00 nM
IC_{50}, [RGD-Glu-[DO3A]-6-Ahx-RM2], U87-MG	321±82.0 nM
IC_{50}, [RGD-Glu-[[^{nat}Y]Y-DO3A]-6-Ahx-RM2], U87-MG	346±5.30 nM

TABLE 2

Biodistribution studies of [RGD-Glu-[[^{90}Y]Y-DO3A]-6-Ahx-RM2] in PC-3 tumor-bearing SCID mice at 1, 4 and 24 h p.i. (%ID/g ± SD, n = 5). Tumor-to-non target tissue ratios for specific organs are in parentheses and italics (%ID/g, n = 5).

	1 h	**4 h**	**24 h**
Heart	0.31±0.06	0.16±0.05	0.15±0.04
Lung	0.80±0.27	0.44±0.06	0.37±0.10
Liver	0.39±0.08 (*22.31*)	0.35±0.07 (*12.80*)	0.29±0.15 (*18.21*)
Kidneys	2.36±0.49 (*3.69*)	1.54±0.31 (*2.91*)	0.89±0.21 (*5.93*)
Spleen	1.36±0.25	1.07±0.18	1.21±0.23
Stomach	1.19±0.34	0.33±0.07	0.22±0.03
S.Intestine	1.41±0.32	0.39±0.09	0.34±0.07
L.Intestine	0.64±0.12	0.66±0.26	0.31±0.06
Muscle	0.22±0.06 (*39.55*)	0.11±0.02 (*40.73*)	0.10±0.03 (*52.80*)
Bone	0.45±0.08	0.29±0.05	0.33±0.12
Brain	0.03±0.01	0.01±0.00	0.00±0.01
Pancreas	6.81±0.92 (*1.28*)	0.55±0.12 (*8.15*)	0.27±0.05 (*19.56*)
Blood *	0.18±0.04 (48.33)	0.01±0.00 (448.0)	0.01±0.00 (528.0)
Urine *	84.6±3.52	93.4±1.26	92.7±2.06
Tumor	8.70±0.35	4.48±0.31	5.28±0.12

* Data presented as %ID